

## Experimental and Theoretical Study to Evaluate the Previous Studies for Expansive Soils

Ahmed S.A. Al-Gharbawi<sup>\*</sup>, Khalid W. Abd Al-Kaream, Mudhafar K. Hameedi, Zainab H. Shakir

Civil Engineering Department, University of Technology-Iraq, Baghdad 00964, Iraq

Corresponding Author Email: [ahmed.s.algharbawi@uotechnology.edu.iq](mailto:ahmed.s.algharbawi@uotechnology.edu.iq)



<https://doi.org/10.18280/mmep.100528>

### ABSTRACT

**Received:** 20 March 2023

**Revised:** 10 May 2023

**Accepted:** 21 May 2023

**Available online:** 27 October 2023

#### Keywords:

*expansive soil, bentonite, empirical equations, free swelling, swelling pressure*

Expansive soils, characterized by their propensity to undergo volume changes in response to moisture variations, pose significant challenges to civil engineering due to the presence of the montmorillonite mineral. This mineral exhibits a high capacity for water absorption, leading to volumetric expansion and consequent soil heave. This study aims to provide a comprehensive understanding of the behavior of expansive soils, focusing on variations induced by different proportions of bentonite enrichment. In this research, both experimental and theoretical approaches are employed. Experimentally, the swell percentage, liquid limit, plastic limit, shrinkage limit, maximum dry density, and optimum moisture content are determined for three bentonite-enriched soil samples: clay with 40%, 60%, and 80% bentonite. Theoretically, the validity of existing empirical equations is assessed in light of the experimentally observed behavior of the bentonite-enriched soils. This dual approach allows for a nuanced understanding of the behavior of expansive soils and provides a foundation for the development of more accurate predictive models. Through this integrated analysis, this study contributes to the body of knowledge on the impact of expansive soils on civil engineering structures and offers a pathway towards more effective management of these challenges.

## 1. INTRODUCTION

Clay, a fine-grained natural soil primarily composed of clay minerals, represents a significant component of the earth's crust. These hydrous aluminum phyllosilicates might contain other elements such as magnesium, iron, and alkali metals. Two notable types of clay are bentonite and montmorillonite, which, despite their frequent interchangeable use, fundamentally differ in their chemical compositions. Bentonite is a clay predominantly constituted by sodium montmorillonite, while montmorillonite clay chiefly comprises sodium or calcium montmorillonite mineral crystals [1-4].

Among these, a particular category of soil – expansive soil – displays substantial volume changes in response to moisture content fluctuations. When hydrated, such soil expands, becoming sticky and heavy due to significant water absorption. Conversely, upon dehydration, it contracts, hardens, and often results in surface cracks up to 20 mm wide [1-4].

Structures erected on expansive soil face potential risks due to the soil's cyclical hardening-softening behavior. This could lead to structural damage in civil infrastructure, such as transportation systems, water supply networks, sewage systems, and residential, commercial, and industrial buildings [5]. Failures occur when volume changes are unevenly distributed beneath a structure's foundation, leading to either end lift or center lift failures, depending on the location of the change in soil water content [5]. The thick, brittle strata beneath the foundation was to blame for the significant settlements [6].

Expansive soil behavior is primarily attributed to its

swelling potential, which poses significant challenges to structural stability due to the consequential heave and differential settlements [7]. Clay particles, characterized by their plate-like shape, can arrange themselves in various ways. Some particles demonstrate a remarkable tendency to adsorb water molecules on their surfaces due to the polar nature of water molecules [8]. This adsorption leads to the formation of a charged fluid film around each particle, resulting in a "double layer phenomenon" where clay particles repel each other, causing the observed swell or heave in expansive soil with increased moisture content.

The liquid limit and plastic limit indices of cohesive soils provide a measure of their ability to attract and adsorb water molecules. Among various clay minerals, montmorillonite clays exhibit the highest swelling potential, whereas kaolinite clays display minimal swelling [9, 10].

Clay minerals are often divided into three main types for engineering purposes:

- i. Kaolinite, which is non-expansive,
- ii. Mica, which includes illites, vermiculites, and chlorites, can be expansive, but usually, do not pose substantial structural problems,
- iii. Smectite, including montmorillonites, are highly expansive and pose the most significant challenges [11].

The application of cohesive non-swelling soil cushions is a broadly utilized technique for enhancing slopes and subgrades in regions with expansive soil. However, the underlying mechanics of how a cohesive non-swelling soil layer can mitigate the impact of expansive soil are yet to be thoroughly elucidated. To deepen our understanding of this inhibitory effect under unidirectional seepage conditions, we have

conducted four outdoor model tests exploring various types of upper layers and thickness. Continuous measurements of soil pressure, electrical resistivity, and swelling deformation were recorded throughout the saturation process. It was observed that when a cohesive, non-swelling soil layer was placed atop an expansive soil layer, there was a marked decrease in the swelling deformation and electrical resistance of the expansive soil layer, especially in the upper half. An increase in the thickness of the cohesive non-swelling soil layer correspondingly enhanced its inhibitory effect [12].

Expansive soil, which expands and contracts in response to moisture content variations, poses a significant risk to civil infrastructure, causing substantial economic losses annually. This type of soil is prevalent in many regions worldwide. Several techniques have been employed to identify the minerals present in expansive soil and to quantify their expansivity. Montmorillonite emerges as a primary constituent of these soils. However, previous studies have not sufficiently addressed the impact of hydrocarbon pollution on the geotechnical properties of expansive soils, necessitating further research in this area [13].

Expansive soil's mechanical properties, characterized by high instability and water sensitivity, can lead to severe engineering mishaps. To determine the quantitative correlation between moisture content and shear strength, cohesiveness, and the internal friction angle, three sets of direct shear experiments were carried out. In order to investigate how cohesion and the internal friction angle affect the maximum amount of displacement and the maximum moment of bending of piles, finite element analysis was used. As moisture content increased, shear strength and matrix suction decreased, while cohesiveness and the internal friction angle increased exponentially. For non-equal length double-row piles, it was discovered that cohesion and internal friction angle had an opposite relationship to the maximum displacement and moment of bending [14].

Expansive soils pose a considerable threat to roads and other lightweight structures, causing damage over time due to their high heave potential, which leads to cracking and swelling [15]. As water seeps into the soil as a result of rapid raising of the subgrade beneath roadways and foundations, roads, floors, and walls may develop cracks. The risks associated with such soils can be mitigated using soil stabilization techniques, which encompass any physical, chemical, or biological methods or combinations thereof employed to improve or alter the properties of natural soil, thereby making it suitable for specific engineering tasks [16].

The active zone, also referred to as the seasonal zone, is a region where soil moisture content fluctuates due to precipitation or evapotranspiration, corresponding with climatic or seasonal changes. The proximity of this zone to the surface means that a larger soil portion experiences swelling phenomena with increasing active zone depth [17]. Typically ranging between 1 and 4 meters, the depth of the active zone, or depth of desiccation, is influenced by soil type, soil structure, terrain, and climate.

Evaluating the swelling behavior of these soils is critical, particularly as lightweight structures with foundation pressures lower than the swelling pressure can exhibit issues such as cracking walls and sticking doors and windows [18]. Numerous techniques have been developed to calculate potential swell in clay and explore the characteristics and behavior of such soil under field-like conditions. These procedures can be broadly classified into two main categories.

## 1.1 Direct methods

An easy laboratory test to gauge the degree of swelling pressure in soils was presented by Das [19] which is the "oedometer test". Water is then introduced to the specimen to cause an expansion in the volume of the soil specimen monitored until equilibrium is attained after the sample is first placed in the oedometer cell under a small surcharge of approximately 6.9 kN/m<sup>2</sup>. It is possible to express the amount of free swell as a ratio:

$$S_{w(free)} (%) = \frac{\Delta H}{H} \times 100 \quad (1)$$

where,

$S_{w(free)}$ : free swell as a percentage.

$\Delta H$ : change in height of swell due to saturation.

$H$ : original height of the specimen.

## 1.2 Indirect methods

Express methods, based on empirical correlations, related to physical properties such as Atterberg limits, mud content, initial moisture content, and dry unit weight. Table 1 below shows the methods used for this.

Soil stability is crucial for expansive soils to have less of a probability of expanding [20]. The goal of chemical stabilization is to provide chemicals that change the liquid limit and plastic limit, respectively, in addition to the plasticity index, which is lowered as a result of the constraints on the liquid and plastic [21]. It improves the soil's workability, moisture content, and maximum dry density as a result of the stabilizing soil's increased compressibility.

For improving the engineering characteristics of swelling soil by employing polypropylene fibers. In this study, the moisture density of soil treated with polypropylene fibers at concentrations of 0, 0.2, 0.4, 0.6, and 0.8% was compared to the elastic modulus, California bearing ratio (CBR), unconfined compressive strength, and one-dimensional consolidation behavior. The lighter fibers replaced the heavier soil particles, drastically reducing the highest possible dry density of reinforced soil by 2.8%, while largely maintaining the appropriate moisture content due to the fibers' non-absorbent properties. The soil that had 0.4% fibers added to it demonstrated significant improvements in its unconfined compressive strength (an improvement of 279%), elastic modulus (an increase of 113.6%), and CBR value (an increase of 94.4% under dry density conditions and an increase of 55.6% under wet conditions), making it a more suitable subgrade for the construction of pavements on such soils. The addition of 0.8% fibers also resulted in a significant reduction in the soil's free swell and swell pressure (94.4% and 87.9%, respectively), ultimately lowering the soil's swelling class from medium to low [22].

**Table 1.** The indirect method was used

Method	Equation
[23]	% swell = $\frac{1}{6.3} \times (S.I)^{1.17}$
[24]	% swell = $3.6 \times 10^{-5} \times A \times 2.44 \times C \times 7.44$
[25]	% swell = $41.13 \times 10^{-5} (S.I) \times 2.67$
[26]	% swell = $(2.29 \times 10^{-2}) (P.I) \times 1.45 \frac{c}{mi} + 6.38$
[27]	log (Sp) = $0.0526 \gamma_{di} + 0.033 L.L - 6.8$
[28]	% swell = $2.2 \times 10^{-5} \times A \times 2.437 \times C \times 3.44$
[29]	Log Ps = $0.782 - 0.0043(wi) + 0.0617(\gamma_d) + 0.0096(LL)$

The objective of this study is to evaluate the empirical equations from the previous study to calculate the free swelling and swelling pressure according to the large time of their studies on expansive. The evaluation was made by using several laboratory tests.

## 2. MATERIALS

### 2.1 Soil characterization

The soil used in this project is brought from the south of Baghdad city and the physical and chemical properties and grain size distribution are in Table 2 and Figure 1, respectively.

**Table 2.** Physical and chemical properties of natural soil

Property	Value
Nature water content (w.c%)	20
Liquid limit (L.L%)	44
Plastic limit (P.L%)	19
Plasticity index (P.I%)	25
Specific gravity (GS)	2.69
Gravel (>2mm)%	0
Sand (0.06 to 2mm)%	16
Silt (0.005 to 0.06mm)%	34
Clay (less than 0.005mm)%	50
Gypsum content %	6.71
SO <sub>3</sub> content %	3.12
Soil symbols(USCS)	CL

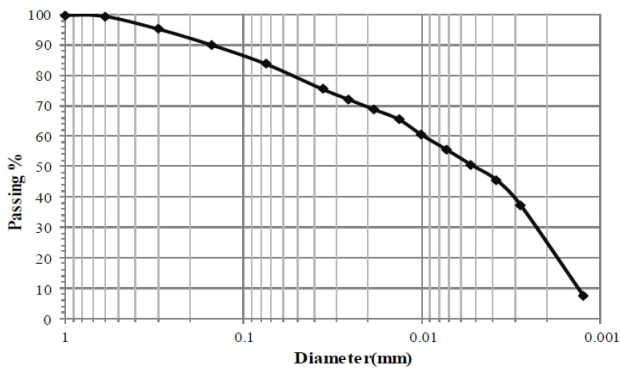


**Figure 1.** Grain size distribution of natural soil

### 2.2 Bentonite characterization

The bentonite used in this project is a commercial Bentonite brought from Saudi Arabia. The properties of this bentonite are shown in Table 3.

**Table 3.** Physical properties of bentonite

Property	Value
Liquid limit (LL %)	512
Plastic limit (PL %)	38
Plasticity index (PI %)	474
Specific gravity (Gs)	2.26

## 3. EXPERIMENTAL WORK

The experimental work includes subjecting the expansive soil to a series of tests aiming at investigating the conduct of expansive soil under the structure.

Generally, the testing program includes two main series. The first series deals with the examination of expansive soil under the effect of structures. In the second series. The information of abbreviating the testing specimens along with naming the sample of models has been illustrated as shown in Figure 2.

Then, this section of work deals with calculating the swelling of the soil at any percentage of bentonite, test data were then analogized using SPSS software V.26.

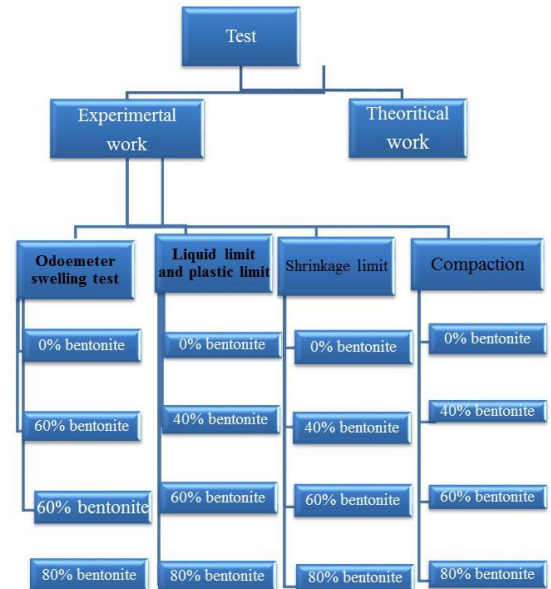


**Figure 2.** Testing program

## 4. PRESENTATION AND DISCUSSION TEST RESULT

### 4.1 Laboratory swelling tests

3 samples of odometer cells are tested to calculate the swelling and swelling pressure for 40%, 60%, and 80% bentonite. The swelling potential that is recorded from these tests is 9.2, 12.3, and 17.7% for 40, 60, and 80% bentonite, respectively. And the swelling pressure is calculated at 99.9, 181.5, and 240.1 kPa for 40, 60, and 80% bentonite, respectively. The findings showed that as bentonite % was increased, swelling potential outcomes also increased. This was due to the chemical makeup of expansive soil minerals, which also increased the pressure required to equalize swelling. Figures 3 to 5 for 40, 60, and 80% bentonite, respectively, illustrate the results of the consolidation tests obtained from the odometer test.

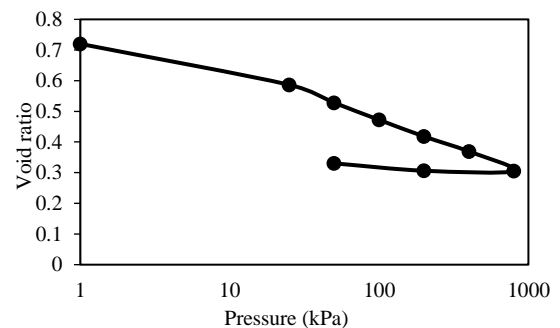


**Figure 3.** Consolidation test for 40% bentonite

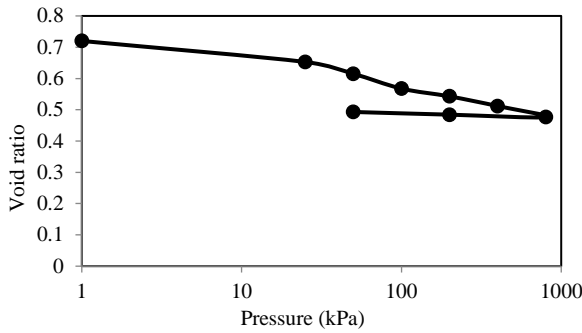


Figure 4. Consolidation test for 60% bentonite

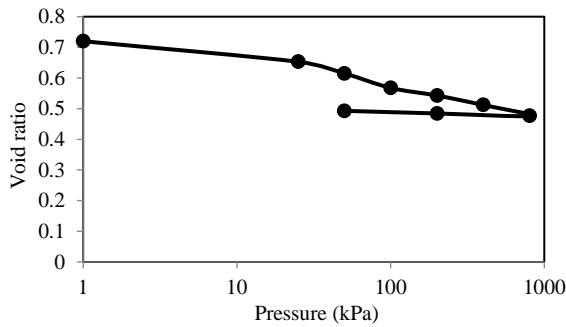


Figure 5. Consolidation test for 80% bentonite

#### 4.2 Atterberg limits

There are 4 samples tested to record Atterberg limits for 0, 40, 60 and 80% bentonite. The results showed that the liquid and plastic limits increase rapidly with the increase in the percentage of bentonite, while the limit of shrinkage increases very simply with the increase in the percentage of bentonite, as a result of the transformation of clay soil into expansive soil that caused this increase in the liquid limit. Table 4 is the summary of laboratory results with increasing bentonite percent and Figures 6 to 10.

Table 4. Summary of Atterberg limit laboratory tests

Soil+Bentonite	Swelling (%)	Swell Pressure (kPa)	L.L (%)	P.L (%)	S.L (%)	P.I	S.I
0%	--	--	41	21	18	20	23
40%	9.2	99.9	62	23	18	39	44
60%	12.3	181.5	81	26	19	55	62
80%	17.7	240.1	85	29	20	56	65

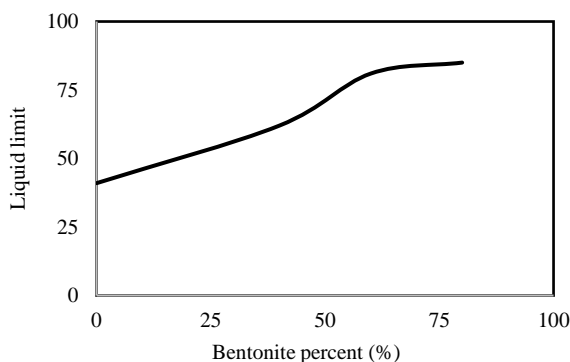


Figure 6. Liquid limit versus bentonite percent

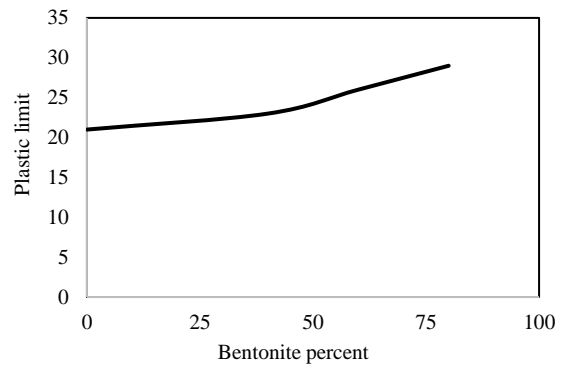


Figure 7. Plastic limit versus bentonite percent

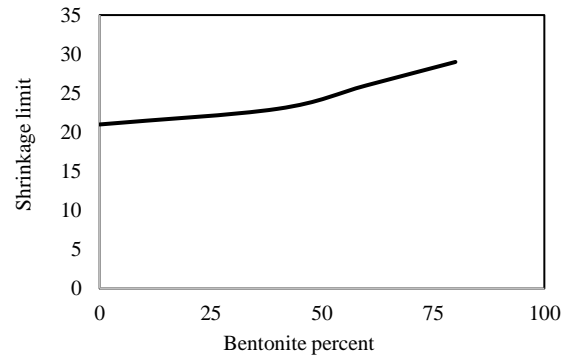


Figure 8. Shrinkage limit versus bentonite percent

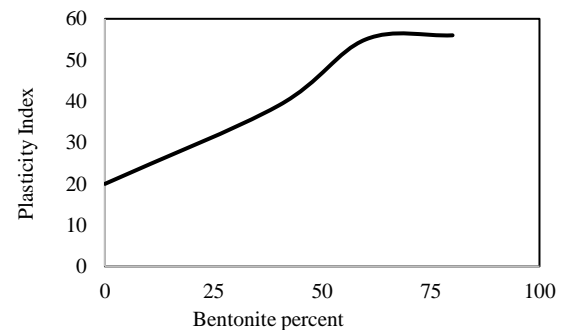


Figure 9. Plasticity index versus bentonite percent

According to the study [30], they summarized that the swelling potential which is can be defined on the basis of the liquid limit, plasticity index, and/or shrinkage limit. They provided tables based on related references for each distinct attribute. Based on the previously mentioned characteristics.

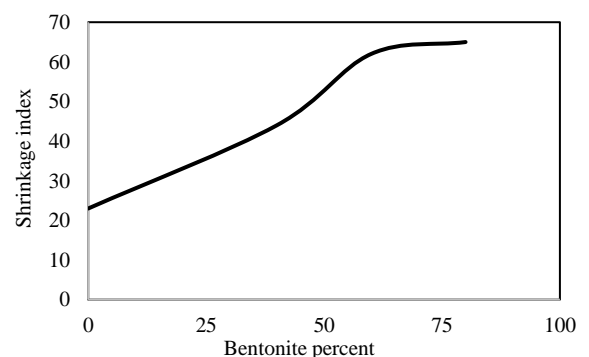


Figure 10. Shrinkage index versus bentonite percent

### 4.3 Compaction test

There are samples tested to calculate the maximum dry unit weight and optimum moisture content for each percent of bentonite. The findings demonstrated that when bentonite concentration grew from 0 to 80%, maximum dry unit weight declined and optimum moisture content increased. This is because swelling soil loses its bearing capacity during heaving [4]. The results of compaction tests are shown in Figures 11 to 14. The summary of compaction laboratory results with increasing bentonite percent is shown in Table 5.

**Table 5.** Summary of laboratory compaction tests

Soil+Bentonite	$\gamma_d$ max.(kN/m <sup>3</sup> )	O.M.C (%)
0%	17.1	17.5
40%	15.1	22.3
60%	14.7	25.1
80%	14.4	27

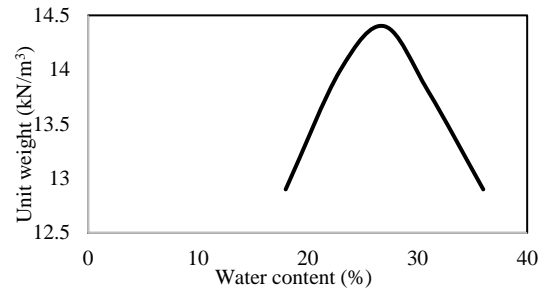


**Figure 14.** Compaction test for 80% bentonite

### 5. ESTIMATION OF SWELLING

To determine the swelling at any percentage of bentonite, test data were then analyzed using the SPSS program. For estimation of settlement and excess pore water pressure in this section. The following equations were found for the soil used.

#### 5.1 Free swelling

For the mathematical equation for free swelling, the results of the tests were chosen. There are three parameters used to extract the free swelling equation in this research: maximum dry unit weight, optimum moisture content, and plasticity index. The free swelling relation is shown in Eq. (2), where  $R^2$  for this equation is 0.89. Figure 15 depicts the mean error analysis, and Figure 16 depicts the findings dissipating.

$$Sw = -298.04 + 10.87 \gamma_{max\ dry} + 8.696 w.c + 1.886 P.I \quad (2)$$

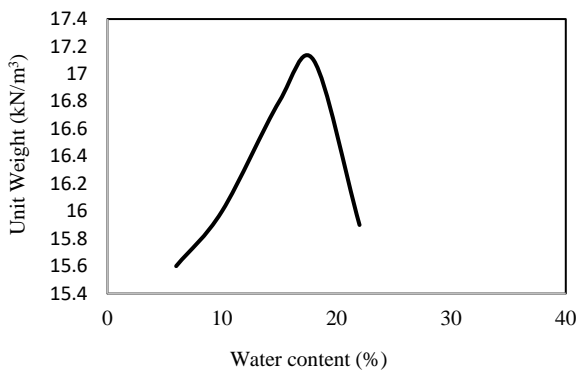


**Figure 11.** Compaction test for 0% bentonite

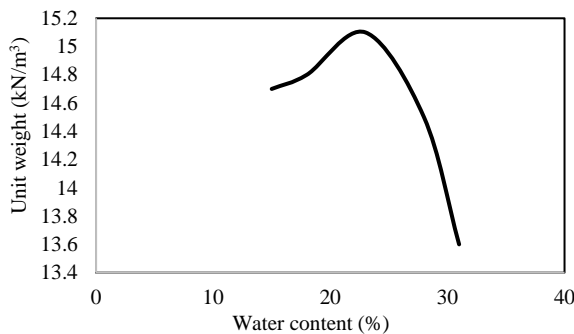


**Figure 12.** Compaction test for 40% bentonite

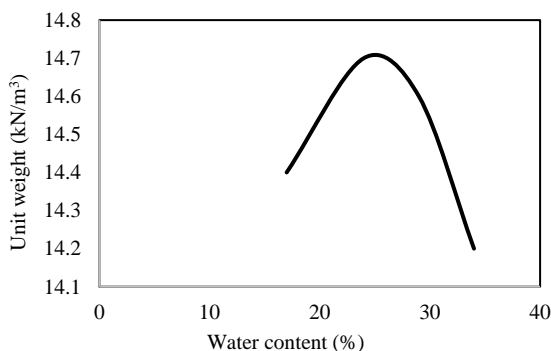


**Figure 13.** Compaction test for 60% bentonite

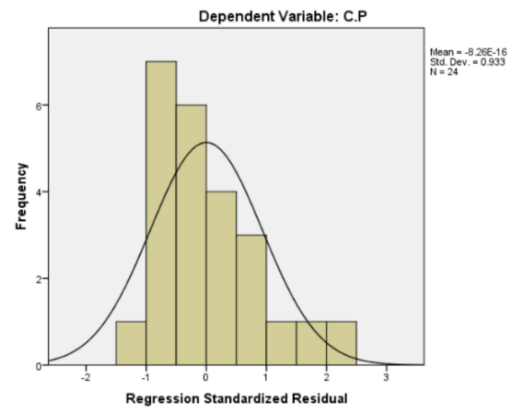


**Figure 15.** Mean error histogram for free swelling

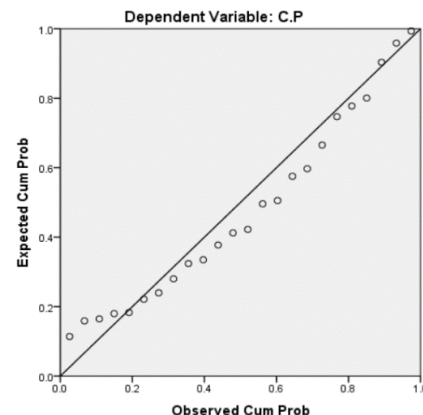


**Figure 16.** Results of dissipation for free swelling

## 5.2 Swelling pressure

For the mathematical equation of swelling pressure, 75% of the result tests are selected randomly and the other 25% are used for checking the equation. There are three parameters used to extract the free swelling equation in this part: the maximum dry unit weight, optimum moisture content, and plasticity index. The relationship of free swelling is shown in Eq. (3), where the R<sup>2</sup> for this equation is 0.9. The mean of error analysis is shown in Figure 17 and the dissipation of the results is shown in Figure 18.

$$Sp = -1.969 + 0.999 w.c + 3.035 \gamma_{max} dry + 0.897 P.I \quad (3)$$

where,

Sp: Swelling pressure.

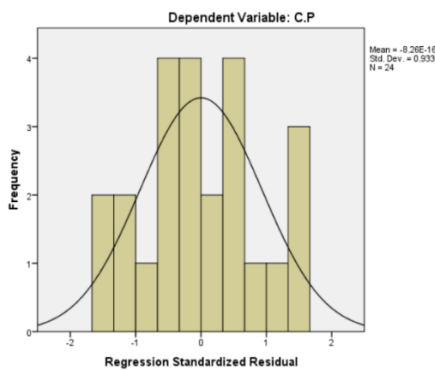


Figure 17. Mean error histogram for swelling pressure

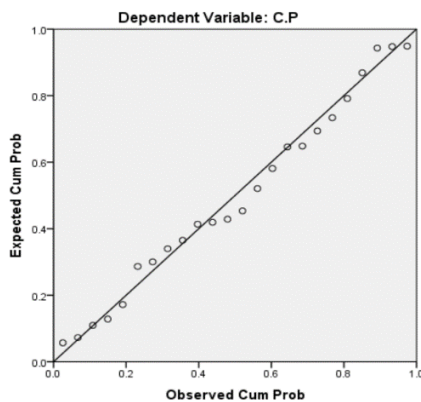


Figure 18. Results of dissipation for swelling pressure

## 6. CONCLUSIONS

Based on the experimental results, the following conclusions can be drawn:

- i. In the experimental swell test, both the free swell and swell pressure escalate rapidly with an increase in bentonite percentage. Specifically, a rise in bentonite percentage from 40% to 80% leads to an approximately 90% increase in free swelling and over a 100% increase in swelling pressure.
- ii. The Atterberg limits demonstrate a significant increase in the liquid limit, plasticity index, and shrinkage index, along with a modest increase in both the plastic limit and shrinkage limit, with a rising bentonite percentage. A surge in bentonite percentage from 40% to 80% results

in about a 37%, 44%, and 48% increase in the liquid limit, plasticity index, and shrinkage index, respectively.

- iii. In terms of the compaction test, there is a decrease in unit weight correlating with an increase in the bentonite percentage, as well as an increase in optimum moisture content.

The predicted values of swelling, compaction, and consistency limit, derived from Eqs. (2)-(3), align excellently with the experimental outcomes. The R<sup>2</sup> values range between 0.89 and 0.9.

## REFERENCES

- [1] Rogers, J.D., Olshansky, R., Rogers, R.B. (1985). Damage to foundation from expansive soil.
- [2] Murthy, V.N.S. (2002). Principles and Practices of Soil Mechanics and Foundation Engineering. New York: Marcek Decker Inc.
- [3] Jones, L.D., Jefferson, I. (2012). Expansive Soils. London, UK, ICE Publishing.
- [4] Al-Gharbawi, A.S., Najemalden, A.M., Fattah, M.Y. (2022). Expansive soil stabilization with lime, cement, and silica fume. Applied Sciences, 13(1): 436. <https://doi.org/10.3390/app13010436>
- [5] Bhavsar, S.N., Joshi, H.B., Shrof, P.K., Patel, A.J. (2014). Effect of burnt brick dust on engineering properties on expansive soil. International Journal of Research in Engineering and Technology, 3(4): 433-441. <https://doi.org/10.15623/ijret.2014.0304078>
- [6] Sánchez, E.R., Esteban, A.M. (2022). Analysis of the G IRALDA tower geotechnical profile and its settlements. International Journal of Computational Methods and Experimental Measurements, 10(1): 1-12. <http://doi.org/10.2495/CMEM-V10-N1-1-12>
- [7] AL-Soudany, K.Y. (2018). Improvement of expansive soil by using silica fume. Kufa Journal of Engineering, 9(1): 222-239. <https://doi.org/10.30572/2018/KJE/090115>
- [8] Coduto, D.P. (2003). Foundation Design on Problematic Soils: Principles and Practices. Prentice-Hall, University of Iowa.
- [9] Al-Showely, J.A. (2014). Piled raft foundations in expansive soils. M.Sc. Thesis, University of Technology-Iraq, Baghdad, Iraq.
- [10] Zeini, H.A., Alabdaly, N.M. (2020). Improving expansive soil properties by adding fuel oil. Journal of Advanced Research in Fluid Mechanics and Thermal Sciences, 70(1): 136-143. <https://doi.org/10.37934/arfmts.70.1.136143>
- [11] Nelson, J., Miller, D.J. (1997). Expansive Soils: Problems and Practice in Foundation and Pavement Engineering. John Wiley & Sons.
- [12] Lucian, C. (2006). Geotechnical aspects of buildings on expansive soils in Kibaha, Tanzania: Preliminary study. Ph.D. Thesis, Department of Civil and Environmental Engineering, Stockholm, Sweden.
- [13] Asghari-Kaljahi, E., Barzegari, G., Jalali-Milani, S. (2019). Assessment of the swelling potential of Baghmisheh marls in Tabriz, Iran. Geomechanics and Engineering, An International Journal, 18(3): 267-275. <https://doi.org/10.12989/gae.2019.18.3.267>
- [14] Wei, M., Liao, F., Zhou, K., Yan, S., Liu, J., Wang, P. (2022). Influence of moisture content on main

- mechanical properties of expansive soil and deformation of non-equal-length double-row piles: A case study. *Geomechanics and Engineering, An International Journal*, 30(2): 139-151. <https://doi.org/10.12989/gae.2022.30.2.139>
- [15] Masood, G.G., Mohammed, H.A., Afaj, H.A.H., Fattah, M.Y. (2021). Behavior of flexible pavement on swelling subgrade soil reinforced with geogrid. *Archives of Civil Engineering*, 67(4): 393-402. <https://doi.org/10.24425/ace.2021.138507>
- [16] Tiwari, K., Sahil S.K., Jatale, A. (2012). Performance, problems and remedial measures for the structures constructed on expansive soil in Malwa Region, India. *International Journal of Emerging Technology and Advanced Engineering*, 2(12): 626-631.
- [17] Lucian, C. (2006). Geotechnical aspects of buildings on expansive soils in Kibaha, Tanzania: Preliminary study. Ph.D. Thesis, Department of Civil and Environmental Engineering, Stockholm, Sweden.
- [18] Thomas, A., Tripathi, R.K., Yadu, L.K. (2019). Alkali-activated GGBS and enzyme on the swelling properties of sulfate bearing soil. *Geomechanics and Engineering, An International Journal*, 19(1): 21-28. <https://doi.org/10.12989/gae.2019.19.1.021>
- [19] Das, M. (2004). *Shallow Foundations- Bearing Capacity and Settlement*. 4th Edition, McGraw-Hill Book Company, London.
- [20] Soundara, B., Selvakumar, S. (2019). Swelling behaviour of expansive soils randomly mixed with recycled geobeads inclusion. *SN Applied Sciences*, 1(10). <https://doi.org/10.1007/s42452-019-1324-4>
- [21] Indiramma, P., Sudharani, C., Needhidasan, S., (2020). Utilization of fly ash and lime to stabilize the expansive soil and to sustain pollution free environment – An experimental study. *Materials Today: Proceedings*, 22: 694-700. <https://doi.org/10.1016/J.MATPR.2019.09.147>
- [22] Ali, M., Aziz, M., Hamza, M., Madni, M.F. (2020). Engineering properties of expansive soil treated with polypropylene fibers. *Geomechanics and Engineering, An International Journal*, 22(3): 227-236. <https://doi.org/10.12989/gae.2020.22.3.227>
- [23] Holtz, W.G., Gibbs, H.J. (1956). Engineering properties of expansive clays. *Transactions of the American Society of Civil Engineers*, 121(1): 641-663. <https://doi.org/10.1061/TACEAT.0007325>
- [24] Seed, H.B., Woodward, R.J., Lundgren, R. (1962). Prediction of swelling potential for compacted clays. *Journal of the Soil Mechanics and Foundations Division*, 88(3): 53-87. <https://doi.org/10.1061/JSFEAQ.0000431>
- [25] Chen, F.H. (1988). *Foundations on Expansive Soils. Developments in Geotechnical Engineering*, Elsevier Publications, the Netherlands.
- [26] Moore, D.M., Reynolds, R.C. (1997). X-ray diffraction and the identification and analysis of clay minerals. *Clay Minerals*, 34(1): 210-211.
- [27] Lu, Z., Tang, C., Yao, H., She, J., Cheng, M., Qiu, Y., Zhao, Y. (2022). Model tests for the inhibition effects of cohesive non-swelling soil layer on expansive soil. *Geomechanics and Engineering, An International Journal*, 29(1): 91-97. <https://doi.org/10.12989/gae.2022.29.1.091>
- [28] Razvi, S.S., Deepak, N., Shubham, B., Atul, Y., Hatim, S., Satyam, B. (2018). Study on stabilization of soil using burnt brick. *International Research Journal of Engineering and Technology (IRJET)*, 5(5).
- [29] Wilson, C.R., Davis, J.G., Mejia, N. (2003). *Landscaping on Expansive Soils*. Colorado State University, U.S. Department of Agriculture and Colorado Counties Cooperating.
- [30] *Motorola Semiconductor Data Manual*. (1989). Motorola Semiconductor Products Inc., Phoenix, USA.

## NOMENCLATURE

Gs	Specific gravity
H	Original high of the specimen
SP	Swelling pressure
SPSS	Statistic package to the Social Science
SL	Shrinkage limit
SI	Shrinkage index
LL	Liquid limit
O.M.C	Optimum moisture content
PL	Plastic limit
SW	Well graded sand
W.C	Water content

## Greek symbols

$\gamma_{max}$	Maximum dry density
$\Delta H$	Change the height of the specimen